

## Crystal Structure, Hirshfeld Surface and Frontier Molecular Orbital Analyses of *N*-[2-(trifluoromethyl)phenyl]succinamic Acid

P.A. SUCHETAN<sup>1,\*</sup>, S. NAVEEN<sup>2</sup>, N.K. LOKANATH<sup>3</sup>, P. KRISHNA MURTHY<sup>4</sup> and M.V. DEEPA URS<sup>5</sup>

<sup>1</sup>Department of Studies and Research in Chemistry, University College of Science, Tumkur University, Tumkur-572103, India

<sup>2</sup>Department of Physics, Faculty of Engineering & Technology, JAIN (Deemed-to-be University), Jain Global Campus, Ramanagera 562 112, India

<sup>3</sup>Department of Studies in Physics, University of Mysore, Manasagangotri, Mysuru-570006, India

<sup>4</sup>Department of Chemistry, Bapatla Engineering College (Autonomous), Bapatla-522101, India

<sup>5</sup>Department of Physics, The National Institute of Engineering, Mysuru-570008, India

\*Corresponding author: E-mail: pasuchetan@gmail.com

Received: 16 June 2020;

Accepted: 20 October 2020;

Published online: 7 December 2020;

AJC-20158

The *ortho*-CF<sub>3</sub> substituent and the N-H bond are in *syn*-conformation in *N*-[2-(trifluoromethyl)phenyl]succinamic acid. In amide and acid functionalities, the carbonyl groups are directed in opposite directions to each other and their related-CH<sub>2</sub> groups. *syn*-Conformation is observed for the acid functionality, where the carbonyl C=O and hydroxyl O-H bonds are directed in the same direction. Three planar fragments comprise of the molecule: aromatic ring (A), core portion -C<sub>arm</sub>-N(H)-C(=O)-C(H<sub>2</sub>)-C(H<sub>2</sub>)(B) and -C(H<sub>2</sub>)-C(=O)-OH(C). The dihedral angle between a pair of fragments being 48.6(4)° (A and B), 81.6 (4)° (B and C) and 70.5 (5)° (A and C). N-H...O hydrogen bonds bind the molecules forming C(4) chains in the crystal, and the neighbouring anti-parallel chains are bound by O-H...O hydrogen bonds resulting in a chair shaped ribbon of one-dimensional nature. The Hirshfeld surface study was carried out, including fingerprint plots. Studies have shown that the interactions with O...H/H...O (27.4%), H...H (27.3%) and H...F/F...H (20.2%) substantially added to the surface. Theoretically, the highest occupied molecular orbital (HOMO), lowest unoccupied molecular orbital (LUMO) and various global reactivity descriptors were also computed by the density functional theory (DFT/B3LYP) approach with a 6-311G(d, p) basis set in the ground state on the geometrically optimized structure in the gas phase.

**Keywords:** Succinamic acid, X-Ray diffraction, Crystal structure, Hydrogen bonds, DFT calculations, Hirshfeld Surfaces.

### INTRODUCTION

Both antitumor and anti-inflammatory activities are shown by substituted succinamic acids [1-4]. As starting materials, they are also very helpful, particularly for the synthesis of *N,N'*-diaryl succinamides, a family of molecules exhibiting a number of biological activities, such as anti-mycobacterial [5], anti-algal [5] and anti-tumor [6].

Hirshfeld surface analyses are essential for the study of modes of packing and re-assurance of the different intermolecular interactions, especially in the molecular crystals [7-9]. It gives a visual illustration in a crystalline environment of intermolecular interactions and molecular shape. Each type of intermolecular atomic and atomic contacts can be identified by their typical surface characteristics. Colour coded distances

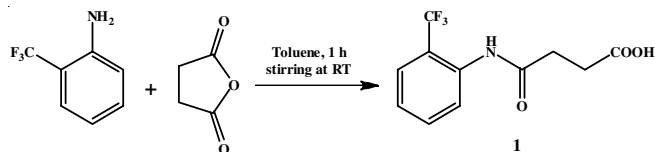
from the closest atom outside the surface to the surface ( $d_e$  plots) and closest atoms inside the surface ( $d_i$  plots) provide a diagrammatic illustration of the numerous modes of interactions present in the crystal. The relative contributions made by each interactions between the molecules in the crystal can also be well illustrated. Especially, the analysis of total 2D fingerprint plot and the fingerprint for the particular atom and atom contacts in a crystal gives information on the percentage contribution made to the Hirshfeld surface by each of the intermolecular contacts experienced by bulk molecules. The demonstration of these in an helpful colour graphic makes it more convenient and useful. To demonstrate the modes of packing and intermolecular interactions encountered by the molecules in the crystal setting, Hirshfeld surfaces consisting of  $d_{norm}$  surfaces and fingerprint were produced and analyzed for the title molecule.

Density functional theory (DFT) is an extremely useful methodology in many fields for performing powerful and inexpensive computational studies [10-13]. For the analysis of structures consisting of electron lone pairs and/or comprehensive electron conjugation [14-17], DFT calculations incorporating the hybrid exchange correlation feature B3LYP (Becke's three parameter (B3) exchange in conjunction with the Lee-Yang-Parr (LYP) correlation function are of special significance. Computational molecular simulation is already an evidently inevitable way to test and forecast the numerous properties of molecules and structures [18,19]. In this work, DFT calculations were used to address descriptors of global reactivity.

Considering the diversified uses of succinamic acids with various substituents and their variants, especially their biological applications, it is worthwhile to synthesize and study the crystal structure of a novel succinamic acid derivative, namely *N*-[2-(trifluoromethyl)phenyl]succinamic acid. The present study was also conducted to illustrate the modifications in the structure- both molecular and crystal that can be obtained on by inserting various substituents to the phenyl ring of *N*-(phenyl)-succinamic acid, which was previously reported [20].

## EXPERIMENTAL

**Synthesis of *N*-[2-(trifluoromethyl)phenyl]succinamic acid:** 2-(Trifluoromethyl)aniline (0.0025 mol, 0.403 g) (15 mL) was dissolved in toluene and mildly heated with constant stirring. To this solution, a hot toluene solution (10 mL) of succinic anhydride (0.0025 mol, 0.25 g) was added dropwise with continuous stirring (**Scheme-I**). Solid title compound was segregated instantly from the solution during the addition. Stirring was performed for 1 h and filtered. To the solid thus obtained was added dil. HCl (10 mL) to separate the unreacted aniline from the title compound solid. The mixture was again filtered under suction and the filtered solid was thoroughly washed with water. The product obtained was recrystallized from ethanol using slow evaporation technique to obtain the colourless product (yield = 0.28 g, 43%; m.p. = 428 K).



**Scheme-I:** Synthesis of *N*-[2-(trifluoromethyl)phenyl]succinamic acid

**X-Ray crystallographic study:** The intensity data of the X-rays diffracted from the single crystal of compound **I** were obtained using 0.71073 Å wavelength radiation (Mo-K $\alpha$ ) at 296 K. The data were collected on a Bruker Proteum2 CCD diffractometer. The diffractometer was equipped with an X-ray generator that operated at 45 kV and 10 mA. The diffracted X-ray intensity data were collected in such a way so as to collect 24 frames per series for different  $\phi$  (0° and 90°) conditions, keeping 0.5° scan width, 5 s exposure time, 45.10 mm gap between sample and detector, and 2 $\theta$  value at 55.2°. Processing of images and reduction of data were made using SAINT-Plus

and XPREP [21]. The direct methods in the SHELXT [22] software were used to establish the crystal structure. The non-hydrogen atoms were observed and refined anisotropically in the first-difference Fourier plot. The H atoms were located geometrically. Geometrically placed were the carbon-bound H atoms, with  $C_{\text{aromatic}} - H = 0.93$  Å and  $C_{\text{methylene}} - H = 0.97$  Å. All hydrogen atoms were refined using the riding model  $U_{\text{iso}}(H) = 1.2U_{\text{eq}}(C)$ . The oxygen bound H atom was positioned at defined positions [O-H = 0.82 Å and  $U_{\text{iso}}(H) = 1.5U_{\text{eq}}(O)$ ]. In contrast, the nitrogen bound H atom was located and modeled as riding from differential Fourier maps: N-H = 0.86 Å. Inside the WinGX suite24 package, all the geometric calculations were performed using PLATON [23] within the WinGX suite [24]. The molecular and packaging diagrams were produced using the MERCURY [25] program.

**Hirshfeld surface calculations:** Hirshfeld surface analysis has been used to analyze the intermolecular interactions present in the title molecule and is a helpful tool for determining the surface characteristics of molecules [7-9]. Hirshfeld surfaces and the corresponding fingerprint are unique to each crystal structure and offer information of the surface intermolecular interactions quantitatively. They are obtained using Crystal Explorer [26] software that accepts a cif format structure as an input file. Two distances are specified for every point on the isosurface of Hirshfeld: distance ( $d_e$ ) [distance between the point and the closest nucleus outside the surface], and distance ( $d_i$ ) [distance between the point and the closest nucleus inside the surface]. The normalized contact distance ( $d_{\text{norm}}$ ) is defined on the basis of distances  $d_e$  and  $d_i$ , and is given by

$$d_{\text{norm}} = \frac{(d_i - r_{\text{vdW}})}{r_{\text{vdW}}} + \frac{(d_e - r_{\text{evdW}})}{r_{\text{evdW}}}$$

where  $r_{\text{vdW}}$  and  $r_{\text{evdW}}$  represent the van der Waals radii of the atoms. The negative signed  $d_{\text{norm}}$  values on the colour scale are illustrated by the red colour indicative of those contacts that are shorter than the van der Waals radii. The white colour on the surface represent those points where the intermolecular distances are close to the van der Waals contacts, with  $d_{\text{norm}}$  values equivalent to zero. Conversely, connections with positive  $d_{\text{norm}}$  values are longer than the total of van der Waals radii and coded with blue.

Hirshfeld surface analyses were conducted using Crystal Explorer 3.0 [26] software and fingerprint was plotted. Colour scales were mapped to the  $d_{\text{norm}}$  plots between -0.18 a.u. (blue) and 1.4 a.u. (red). The fingerprint [8] is presented in the expanded view, with the distances  $d_e$  and  $d_i$  in the range 0.6-2.8 Å presented on the graph axes. The hydrogen bond lengths were immediately modified to regular standard neutron values, *i.e.* C-H = 1.083 Å and N-H = 1.009 Å, when the cif file was uploaded into the Crystal Explorer software.

**DFT calculations:** In order to quantify global reactivity parameters such as  $E_{\text{HOMO}}$ ,  $E_{\text{LUMO}}$ ,  $\Delta E(E_{\text{HOMO}} - E_{\text{LUMO}})$ , Electron affinity (A), electronegativity ( $\chi$ ), ionization potential (I), chemical potential ( $\mu$ ), global hardness ( $\eta$ ), chemical softness ( $\omega$ ), electrophilicity index ( $\omega$ ), electron donation power ( $\omega^-$ ) and electron acceptance ( $\omega^+$ ), the optimized geometry in the ground state and gas phase obtained by DFT technique was used. Using

Gaussian 09 software package [27], measurements were made within DFT with B3LYP exchange-correlation hybrid functional [28,29] extended base sets with polarization and diffuse functions 6-311G(d,p). For the processing and visualization of input/output data, the GaussView 5.0.8 software was used.

## RESULTS AND DISCUSSION

**Molecular conformation:** Table-1 shows the crystallographic descriptions of the compound and Table-2 listed the selected bond lengths and bond angles, while the different hydrogen bonds and their geometries are shown in Table-3. The N-H bond in the title molecule's side chain and the *ortho*-CF<sub>3</sub> substituent are in *syn*-conformation (Fig. 1). In comparison, amide and acid carbonyl groups are *anti*-conforming and are even *anti*-conforming to their adjacent CH<sub>2</sub> groups. The O2=C10-O3-H3 torsion angle = 32.6 (9)° shows the *syn*-orientation of the C=O and O-H bonds of the acid group. Three planar fragments compose the molecule-the aromatic ring (A), the center portion C1-N1-C7(=O1)-C8-C9 (B), and C9-C10(=O3)-O3(C). For all the non-H atoms in B, the r.m.s.d. is 0.002 Å, and in C, it is 0.011 Å. The dihedral angle between the three segments taken two at a time is 48.6 (4)° (A and B), 81.6 (4)° (B and C), and 70.5 (5)° (A and C). The -CH<sub>2</sub>-CH<sub>2</sub>- bond in the side chain has staggered conformation.

To date, 47 substituted *N*-(aryl)succinamic acids have been reported. The phenyl rings of the reported structures bear different substituents at different positions (mono-, di- and

TABLE-1  
SINGLE-CRYSTAL DATA AND  
REFINEMENT PARAMETERS FOR (I)

CCDC deposit	1993889
Empirical formula	C <sub>11</sub> H <sub>10</sub> NO <sub>3</sub> F <sub>3</sub>
Formula weight	261.20
Temperature (K)	293(2)
Crystal system	Triclinic
Space group	<i>P</i> -1
a (Å)	4.828(13)
b (Å)	11.46(3)
c (Å)	11.87(3)
α (°)	65.72(6)
β (°)	81.62(8)
γ (°)	84.03(7)
Volume (Å <sup>3</sup> )	592(3)
Z	2
ρ <sub>calc</sub> (g/cm <sup>3</sup> )	1.466
μ (mm <sup>-1</sup> )	0.137
F(000)	268.0
Crystal size (mm <sup>3</sup> )	0.21 × 0.19 × 0.16
Radiation	MoKα (λ = 0.71073)
2θ range for data collection (°)	6.992 to 55.226
Index ranges	-6 ≤ h ≤ 6, -14 ≤ k ≤ 13, -13 ≤ l ≤ 15
Reflections collected	3487
Independent reflections	2663 [R <sub>int</sub> = 0.0525, R <sub>sigma</sub> = 0.1101]
Data/restraints/parameters	2663/1/168
Goodness-of-fit on F <sup>2</sup>	1.029
Final R indexes [I > 2σ(I)]	R <sub>1</sub> = 0.1023, wR <sub>2</sub> = 0.2766
Final R indexes [all data]	R <sub>1</sub> = 0.1981, wR <sub>2</sub> = 0.3425
Largest diff. peak/hole (e Å <sup>-3</sup> )	0.25/-0.25

TABLE-2  
BOND LENGTHS (Å), ANGLES AND  
TORSIONS (°) IN THE TITLE COMPOUND

F1-C11	1.320 (8)	C9-C10	1.492 (9)
F2-C11	1.340 (9)	C9-C8	1.514 (8)
F3-C11	1.317 (8)	C8-C7	1.505 (8)
O2-C10	1.227 (7)	C2-C11	1.495 (9)
O1-C7	1.227 (7)	N1-C7	1.355 (7)
O3-C10	1.314 (7)	N1-C1	1.425 (8)
C7-N1-C1	125.9 (4)	O1-C7-N1	123.4 (5)
C10-C9-C8	112.8 (5)	O1-C7-C8	121.6 (5)
C7-C8-C9	113.6 (5)	N1-C7-C8	114.9 (4)
C3-C2-C11	118.9 (6)	C6-C1-N1	120.1 (5)
C1-C2-C11	121.9 (5)	C2-C1-N1	120.4 (5)
O2-C10-O3	122.1 (6)	O3-C10-C9	113.9 (5)
O2-C10-C9	123.8 (5)		
C10-C9-C8-C7	-72.0 (7)	C1-N1-C7-C8	179.0 (5)
C5-C6-C1-N1	179.1 (5)	C9-C8-C7-O1	-3.6 (9)
C11-C2-C1-C6	-174.4 (5)	C9-C8-C7-N1	177.0 (5)
C3-C2-C1-N1	-178.1 (5)	C11-C2-C3-C4	175.4 (6)
C11-C2-C1-N1	4.5 (8)	C1-N1-C7-O1	-0.3 (9)
C7-N1-C1-C6	48.7 (8)	C8-C9-C10-O2	-21.1 (8)
C7-N1-C1-C2	-130.2 (6)	C8-C9-C10-O3	162.8 (5)

TABLE-3  
LIST OF DIFFERENT HYDROGEN-BONDS AND  
OTHER INTERMOLECULAR INTERACTIONS (Å, °)  
IN THE TITLE COMPOUND'S CRYSTAL STRUCTURE  
AND THEIR GEOMETRIC SPECIFICATIONS

D-H...A	D-H	H...A	D...A	D-H...A
N1-H1...O1 <sup>i</sup>	0.86	2.13	2.9648(10)	165
O3-H3...O2 <sup>ii</sup>	0.82	2.07	2.686(10)	132

i: 1+x,y,z; ii: 1-x, 3-y, 1-z

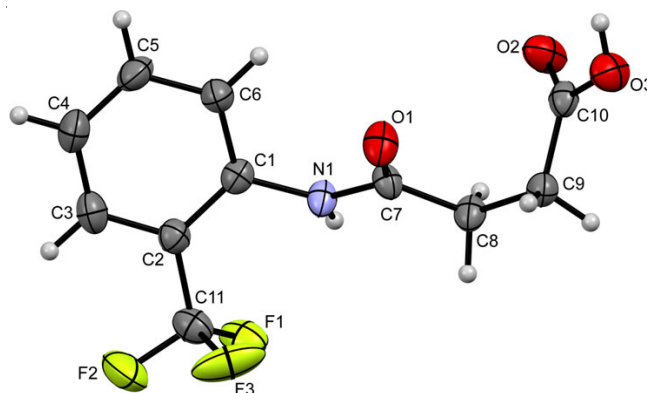


Fig. 1. A view of the molecular structure of compound I in which the thermal ellipsoids are fixed at 50% probability level

trisubstituted derivatives at different positions) and even containing heterocyclic rings. Three of these compounds, *i.e.* *N*-(phenyl)-succinamic acid (CCDC refcode: IJOYEM) [20] and two *ortho*-substituted compounds, *i.e.* *N*-(2-methylphenyl)-succinamic acid [30] and *N*-(2-chlorophenyl)succinamic acid [31], are highly associated with title compound I. Rest of them are the compounds with either di-/tri-substitutions or heterocyclic compounds, or the monosubstituted ones with substitutions at positions other than *ortho*. In addition, the crystal structure of an analogue of I with maleic acid, namely, *N*-[2-(trifluoromethyl)-phenyl]maleamic acid, has recently been described [32].

In all the three corresponding succinamic acids and the analogous maleamic acid, the -COOH group adopts *syn*-conformation identical to that in title compound **I**. In all the three succinamic acids identical to the one in title compound **I**, the conformations of amide and acid carbonyl groups are both *anti*- to each other and even to the adjacent-CH<sub>2</sub> groups. This is identical to that found in *N*-[2-(trifluoromethyl)phenyl]-maleamic acid, where amide and acid carbonyl groups are *anti*- to each other and even to the adjacent -CH groups. The N-H bonds in the side chains of *N*-(2-methylphenyl)succinamic acid, *N*-(2-chlorophenyl)succinamic acid and *N*-[2-(trifluoromethyl)phenyl]-maleamic acid and their *ortho*-substituents are in *syn*-conformation as in title compound **I**. It is found that three corresponding succinamic acids vary from title compound **I** in the way the side chains are oriented with respect to the aromatic ring (Fig. 2).

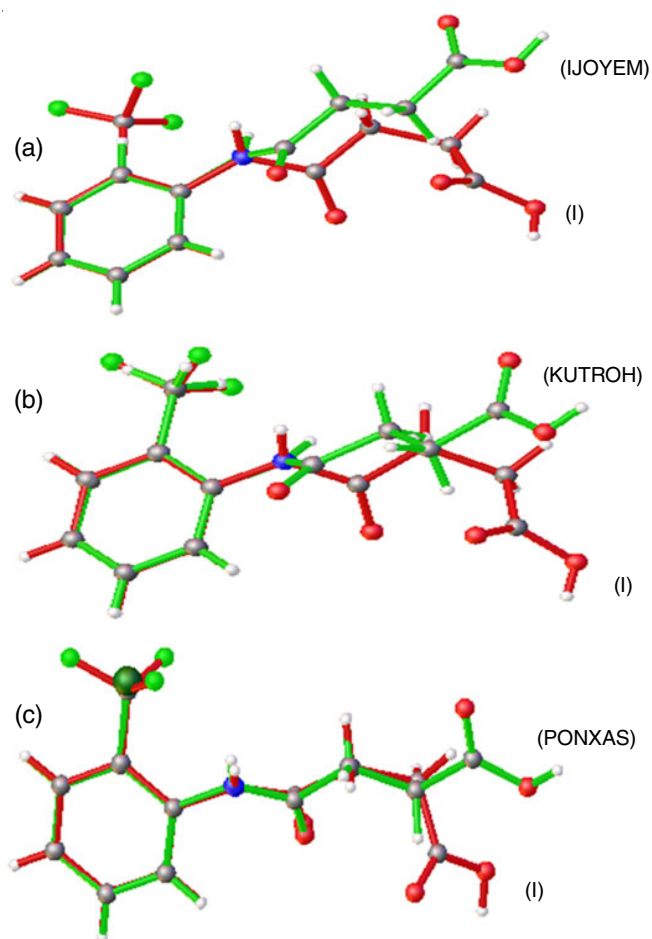


Fig. 2. A view of the molecular fit of compound **I** with (IJOYEM) (a), (KUTROH) (b) and (PONXAS) (c)

**Crystal structure:** The molecules in the crystal of (**I**) are connected through N1-H1...O1 hydrogen bonds that create C<sub>1</sub>(4) chains parallel to the crystallographic *a*-axis (Fig. 3). O3-H3...O2 hydrogen bonds forming inversion-related R<sub>2</sub><sup>2</sup>(8) dimers (Fig. 3) connects the neighboring chains *anti*-parallel to each other, resulting in a chair-shaped ribbon propagating along the *a*-axis. Thus, a one-dimensional chair shaped ribbon ensues.

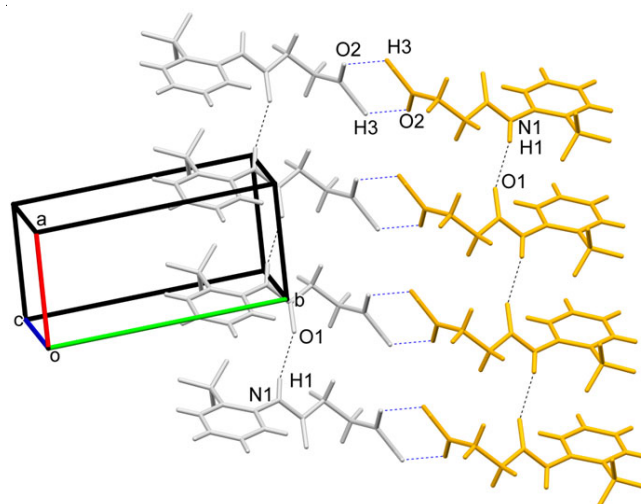


Fig. 3. O-H...O and N-H...O hydrogen-bonded ribbons (thin blue lines) propagating along *a* axis, when viewed approximately down the *c* axis of the crystal packing in compound **I**

The type and motif of hydrogen bonds and intermolecular interactions, and hence, the consequential framework in title compound **I** are identical to those found in the associated succinamic acids as mentioned above. In *N*-[2-(trifluoromethyl)phenyl]maleamic acid, however, two-dimensional sheets formed by O-H...O and N-H...O hydrogen bonds are crosslinked through interactions of the type C-H...O into a 3D network. The packing properties of the two analogues, which vary only in the form of C-C bond in the chain, are also entirely different.

**Hirshfeld surface analysis:** In order to further analyze the intermolecular interactions and hydrogen bonds in the crystal structure of title compound **I** and also to obtain a piece of evidence for the relative quantitative contributions of these to the surfaces, the analyses of Hirshfeld surface mapped over  $d_{\text{norm}}$  surfaces and the two-dimensional fingerprint plots were made [33]. The presence of dark-red spots in the proximities of the O1 and O2 oxygen atoms confirms the involvement of these oxygen atoms as a strong acceptor in hydrogen bonding frameworks (Fig. 4). Likewise, dark-red spots around the hydrogen atoms of H1 and H3 are attributed to their presence in stronger hydrogen bonds as donors (Fig. 4).

The fingerprint features a set of large, pointed spikes typical of strong hydrogen bonds (Fig. 5). The occurrence of pointed spikes at  $d_i + d_e \approx 1.9$  Å in the fingerprint of H...O/O...H contacts almost matches with the  $d_{\text{H...A}}$  value observed for O3-H3...O2 hydrogen bond in the crystal structure (Table-3). The study of the fingerprint shows that the primary contribution to the total Hirshfeld surfaces of title compound **I** consists of O...H/H...O contact (27.4%;  $d_i + d_e \approx 1.9$  Å), followed by H...H (27.3%;  $d_i + d_e \approx 2.4$  Å), F...H/H...F (20.2%;  $d_i + d_e \approx 2.6$  Å), C...H/H...C (6.9%;  $d_i + d_e \approx 2.8$  Å), F...F (6.3%;  $d_i + d_e \approx 3.2$  Å), C...F/F...C (5.7%;  $d_i + d_e \approx 3.2$  Å) and 6.2% by others.

**Optimization of geometry and frontier molecular orbital analysis:** Using the DFT/B3LYP/6-311G(d,p) basis package, the title compound **I** was optimized. The designed structure (Fig. 6) has 0.5975 Debye dipole moment and -1005.47277039

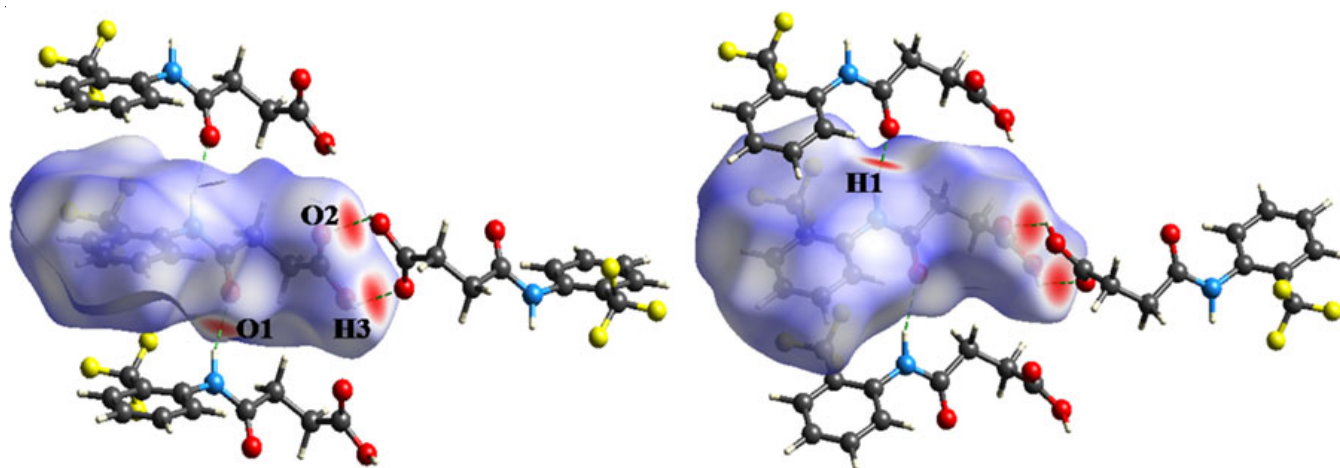


Fig. 4. Hirshfeld surface, mapped over the range  $-0.753$  to  $1.252$  a.u. in the  $d_{\text{norm}}$  for the molecule in compound **I**, displaying its interaction with neighboring molecules *via* hydrogen bonds (dashed lines)

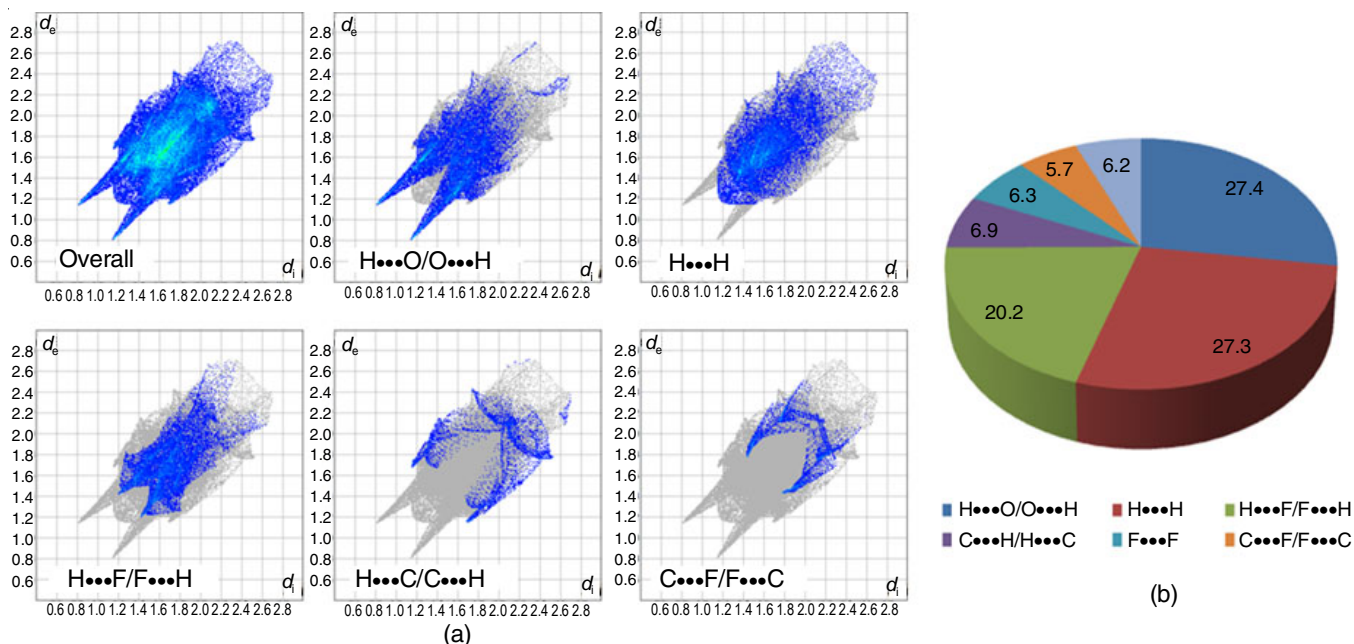


Fig. 5. Total FP and those decomposed into  $\text{O}\cdots\text{H}/\text{H}\cdots\text{O}$ ,  $\text{F}\cdots\text{H}/\text{H}\cdots\text{F}$ ,  $\text{H}\cdots\text{H}$ ,  $\text{C}\cdots\text{H}/\text{H}\cdots\text{C}$  and  $\text{C}\cdots\text{F}/\text{F}\cdots\text{C}$  contacts in compound **I**

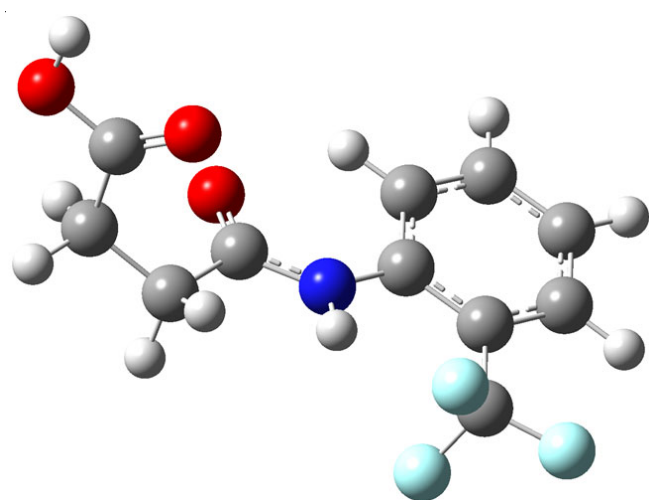


Fig. 6. Optimized structure of the title compound **I**

a.u. ground state energy. The energies of the HOMO and LUMO orbitals for the title compound are  $-6.6240$  and  $-1.1760$  eV, respectively. The molecule-associated global chemical descriptors are: ionization potential ( $I$ ) =  $6.6240$  eV, electron affinity ( $A$ ) =  $1.1760$  eV, electronegativity ( $\chi$ ) =  $7.8$ , global hardness ( $\eta$ ) =  $5.448$ , chemical potential ( $\mu$ ) =  $-7.8$ , electrophilicity index ( $\omega$ ) =  $5.5837$ , electron donation power ( $\omega^-$ ) =  $5.0823$  and electron acceptance value ( $\omega^+$ ) =  $1.1823$  eV [34,35]. It is apparent from Fig. 7 that HOMO is positioned over the phenyl ring, amide group and partly over the  $-\text{CF}_3$  group, and that LUMO is positioned over the phenyl ring, carbonyl and  $-\text{CF}_3$  groups. This indicates the electrons in the molecular system are delocalized.

### Conclusion

Title compound, *N*-[2-(trifluoromethyl)phenyl]succinic acid (**I**), was synthesized and by single-crystal X-ray diffraction

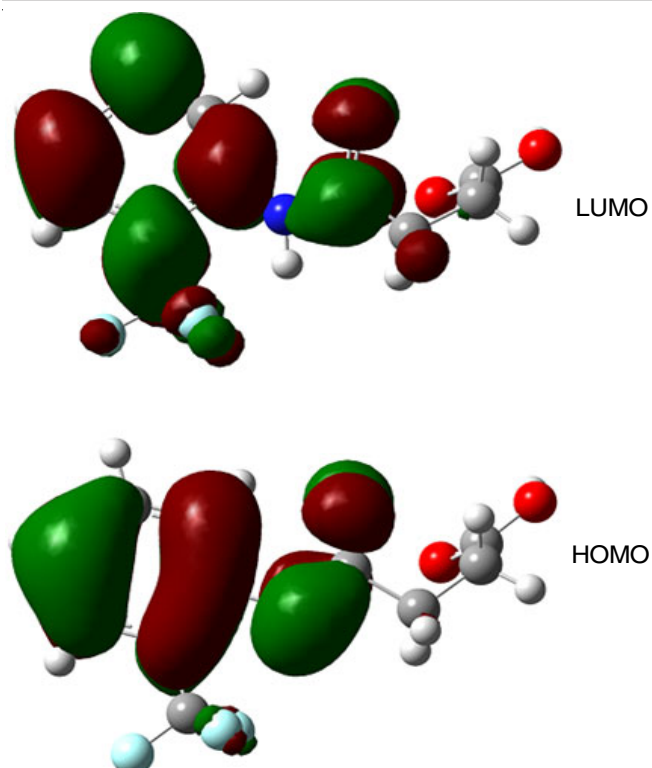


Fig. 7. HOMO and LUMO of *N*-[2-(trifluoromethyl)phenyl]succinamic acid (I)

experimental study, its molecular and crystal structure was determined. In the molecule, substituent  $-CF_3$  at the *ortho* position and the N-H bond are in *syn*-conformation. In comparison, carbonyl groups in the amide and acid functionalities are aligned *anti* to each other and even to the respectively attached methylene groups. Also, the carboxylic acid ( $-COOH$ ) group has *syn*-conformation. Three planar fragments comprise of the molecule *viz.* aromatic ring (A), central portion  $-C_{arm}-N(H)-C(=O)-C(H_2)-C(H_2)(B)$  and  $-C(H_2)-C(=O)-OH(C)$ . The dihedral angles are  $48.6(4)^\circ$  (A and B),  $81.6(4)^\circ$  (B and C), and  $70.5(5)^\circ$  (A and C). Adjacent anti-parallel N-H $\cdots$ O hydrogen bond C(4) chains are connected in the crystal through O-H $\cdots$ O hydrogen bonds forming  $R_2^2(8)$  dimers related by inversion. These ensure a one-dimensional chair shaped ribbon. The Hirshfeld surface fingerprint plots indicate that O $\cdots$ H/H $\cdots$ O contacts (27.4%) led by H $\cdots$ H (27.3 %) and H $\cdots$ F/F $\cdots$ H (20.2%) are the largest contribution to surface contacts. To quantify different global reactivity parameters, the refined geometry in the ground state and gas-phase acquired *via* the DFT technique was used. The spatial distribution of HOMO and LUMO showed the delocalization of electrons inside the molecule. The molecule is correlated with less chemical reactivity and strong kinetic stability as it has a broad HOMO-LUMO energy gap ( $\Delta E$ ) = 5.4480eV.

#### ACKNOWLEDGEMENTS

This article is dedicated to commemorate the 25th year of the National Single Crystal X-Ray Diffractometer Facility at Department of Studies in Physics, Manasagangotri, University of Mysore, Mysuru, India

#### CONFLICT OF INTEREST

The authors declare that there is no conflict of interests regarding the publication of this article.

#### REFERENCES

1. D. Burdulene, A. Palaima, Z. Stumbryavichyute, Z. Talaikite and V. Shimkyavichiene, *Pharm. Chem. J.*, **33**, 125 (1999); <https://doi.org/10.1007/BF02508446>
2. D. Burdulene, Z. Stumbryavichyute, Z. Talaikite, G.V. Vladyko, E.I. Boreko and L.V. Korobchenko, *Pharm. Chem. J.*, **31**, 471 (1997); <https://doi.org/10.1007/BF02464305>
3. D. Burdulene, Z. Stumbryavichyute, Z. Talaikite, G.V. Vladyko, E.I. Boreko and L.V. Korobchenko, *Pharm. Chem. J.*, **30**, 680 (1996); <https://doi.org/10.1007/BF02223742>
4. D. Burdulene, Z. Stumbryavichyute, Z. Talaikite, G.A. Penyazeva, S.L. Buldakova, S.E. Metkalova, E.I. Drozdova, M.M. Olenin, V.A. Luchin and A.D. Shiryaev, *Pharm. Chem. J.*, **29**, 262 (1995); <https://doi.org/10.1007/BF02219550>
5. L. Kubicova, K. Waissner, J. Kunes, K. Kralova, Z. Odlerova, M. Slosarek, J. Janota and Z. Svoboda, *Molecules*, **5**, 714 (2000); <https://doi.org/10.3390/50500714>
6. F. Hadizadeh, A. Moradi, G. Naghibi, M. Vojdani, J. Behravan and M. Ramezani, *Int. J. Biomed. Sci.*, **3**, 60 (2007).
7. S.K. Seth, *J. Mol. Struct.*, **70**, 1064 (2014); <https://doi.org/10.1016/j.molstruc.2014.01.068>
8. M.A. Spackman and J.J. McKinnon, *CrystEngComm*, **4**, 378 (2002); <https://doi.org/10.1039/B203191B>
9. M.A. Spackman, J.J. McKinnon and D. Jayatilaka, *CrystEngComm*, **10**, 377 (2008); <https://doi.org/10.1039/B715227B>
10. A. Maiti, A. Svizhenko and M.P. Anantram, *Phys. Rev. Lett.*, **88**, 1268051 (2002); <https://doi.org/10.1103/PhysRevLett.88.126805>
11. D. Zhou, D. Ma, Y. Wang, X. Liu and X. Bao, *Chem. Phys. Lett.*, **373**, 46 (2003); [https://doi.org/10.1016/S0009-2614\(03\)00513-X](https://doi.org/10.1016/S0009-2614(03)00513-X)
12. J. Leconte, A. Markovits, M.K. Skalli, C. Minot and A. Belmajdoub, *Surf. Sci.*, **497**, 194 (2002); [https://doi.org/10.1016/S0039-6028\(01\)01477-7](https://doi.org/10.1016/S0039-6028(01)01477-7)
13. J.G. Wang, C.J. Liu, Z. Fang, Y. Liu and Z. Han, *J. Phys. Chem. B*, **108**, 1653 (2004); <https://doi.org/10.1021/jp035779o>
14. M.E. Vaschetto, B.A. Retamal and A.P. Monkman, *J. Mol. Struct. THEOCHEM*, **468**, 209 (1999); [https://doi.org/10.1016/S0166-1280\(98\)00624-1](https://doi.org/10.1016/S0166-1280(98)00624-1)
15. T. Clark, J. Chandrasekhar, G.W. Spitznagel and P.V.R. Schleyer, *J. Comput. Chem.*, **4**, 294 (1983); <https://doi.org/10.1002/jcc.540040303>
16. S. Gronert, *Chem. Phys. Lett.*, **252**, 415 (1996); [https://doi.org/10.1016/0009-2614\(96\)00162-5](https://doi.org/10.1016/0009-2614(96)00162-5)
17. D.A. Forsyth and A.B. Sebag, *J. Am. Chem. Soc.*, **119**, 9483 (1997); <https://doi.org/10.1021/ja970112z>
18. S. Armakovic, S.J. Armakovic and S. Koziel, *Carbon*, **111**, 371 (2017); <https://doi.org/10.1016/j.carbon.2016.10.022>
19. S. Armakovic, S.J. Armakovic and B.F. Abramovic, *J. Mol. Model.*, **22**, 240 (2016); <https://doi.org/10.1007/s00894-016-3101-2>
20. B.T. Gowda, S. Foro, B.S. Saraswathi and H. Fuess, *Acta Crystallogr. E*, **67**, o249 (2011); <https://doi.org/10.1107/S160053681005364X>
21. Bruker. APEX2, SAINT-Plus and SADABS. Bruker AXS Inc., Madison, Wisconsin, USA (2004).
22. G.M. Sheldrick, *Acta Crystallogr. A*, **71**, 3 (2015); <https://doi.org/10.1107/S2053273314026370>
23. A.L. Spek, *Acta Crystallogr. A*, **46**, C34 (1990); <https://doi.org/10.1107/S0108767390099780>
24. L.J. Farrugia, *J. Appl. Cryst.*, **45**, 849 (2012); <https://doi.org/10.1107/S0021889812029111>

25. C.F. Macrae, I.J. Bruno, J.A. Chisholm, P.R. Edgington, P. McCabe, E. Pidcock, L. Rodriguez-Monge, R. Taylor, J. van de Streek and P.A. Wood, *J. Appl. Cryst.*, **41**, 466 (2008); <https://doi.org/10.1107/S0021889807067908>
26. S.K. Wolff, D.J. Grimwood, J.J. McKinnon, D. Jayatilaka and M.A. Spackman, Crystal Explorer 3.0, University of Western Australia, Perth, Australia (2001).
27. M.J. Frisch, G.W. Trucks, H.B. Schlegel, G.E. Scuseria, M.A. Robb, J.R. Cheeseman, G. Scalmani, V. Barone, B. Mennucci, G.A. Petersson, H. Nakatsuji, M. Caricato, X. Li, H.P. Hratchian, A.F. Izmaylov, J. Bloino, G. Zheng, J.L. Sonnenberg, M. Hada, M. Ehara, K. Toyota, R. Fukuda, J. Hasegawa, M. Ishida, T. Nakajima, Y. Honda, O. Kitao, H. Nakai, T. Vreven, J.A. Montgomery Jr., J.E. Peralta, F. Ogliaro, M. Bearpark, J.J. Heyd, E. Brothers, K.N. Kudin, V.N. Staroverov, T. Keith, R. Kobayashi, J. Normand, K. Raghavachari, A. Rendell, J.C. Burant, S.S. Iyengar, J. Tomasi, M. Cossi, N. Rega, J.M. Millam, M. Klene, J.E. Knox, J.B. Cross, V. Bakken, C. Adamo, J. Jaramillo, R. Gomperts, R.E. Stratmann, O. Yazyev, A.J. Austin, R. Cammi, C. Pomelli, J.W. Ochterski, R.L. Martin, K. Morokuma, V.G. Zakrzewski, G.A. Voth, P. Salvador, J.J. Dannenberg, S. Dapprich, A.D. Daniels, O. Farkas, J.B. Foresman, J.V. Ortiz, J. Cioslowski and D.J. Fox, Gaussian, Inc., Wallingford CT (2010).
28. C. Lee, W. Yang and R.G. Parr, *Phys. Rev. B Condens. Matter*, **37**, 785 (1988); <https://doi.org/10.1103/PhysRevB.37.785>
29. A.D. Becke, *J. Chem. Phys.*, **98**, 5648 (1993); <https://doi.org/10.1063/1.464913>
30. B.T. Gowda, S. Foro, B.S. Saraswathi and H. Fuess, *Acta Crystallogr. E*, **66**, o908 (2010); <https://doi.org/10.1107/S1600536810010329>
31. B.T. Gowda, S. Foro, B.S. Saraswathi, H. Terao and H. Fuess, *Acta Crystallogr. E*, **65**, o399 (2009); <https://doi.org/10.1107/S1600536809002979>
32. M.S. Krawczyk and I. Majerz, *Acta Crystallogr. E*, **75**, 766 (2019); <https://doi.org/10.1107/S2052520619009065>
33. M.J. Turner, J.J. Mckinnon, S.K. Wolff, D.J. Grimwood and P.R. Spackman, D. Jayatilaka and M. A. Spackman, CrystalExplorer17, The University of Western Australia, Perth, Australia (2017).
34. T.A. Koopmans, *Physica*, **1**, 104 (1934); [https://doi.org/10.1016/S0031-8914\(34\)90011-2](https://doi.org/10.1016/S0031-8914(34)90011-2)
35. R.J. Parr, L.V. Szentpaly and S. Liu, *J. Am. Chem. Soc.*, **121**, 1922 (1999); <https://doi.org/10.1021/ja983494x>